Dynamics of Anilinium Radical α-Heterolytic Fragmentation Processes. Electrofugal Group, Substituent, and Medium Effects on Desilylation, Decarboxylation, and Retro-Aldol Cleavage Pathways

Zhuoyi Su,[†] Patrick S. Mariano,*[,†,1] Daniel E. Falvey,[‡] Ung Chan Yoon,[§] and Sun Wha Oh[§]

Contribution from the Department of Chemistry, University of New Mexico, Albuquerque, New Mexico 87111, Department of Chemistry and Biochemistry, University of Maryland, College Park, Maryland 20742, and Department of Chemistry, College of Natural Sciences, Pusan National University, Pusan 609-735, Korea

Received May 4, 1998

Abstract: A single electron transfer (SET) photosensitization technique in conjunction with time-resolved, laser spectroscopy has been employed to generate and kinetically analyze decay processes of anilinium radicals derived by one-electron oxidation of α-anilinocarboxylates, *β*-anilinoalcohols, and α-anilinosilanes. In this manner, the rates of unimolecular decarboxylation of aniliniumcarboxylate radicals were determined to be in the range 10^6-10^7 s^{-1} and dependent upon solvent polarity, the nature of the metal cation, and substituents on the aniline ring, nitrogen, and α-carbon. In addition, kinetic analysis of base-induced retro-aldol fragmentations of cation radicals arising by SET oxidation of *β*-anilinoalcohols has shown that they occur with bimolecular rate constants which vary from 10^4 to 10^5 M^{-1} s^1. These values are close to those for α-deprotonation reactions of related *N*,*N*-dialkylanilinium radicals. The retro-aldol fragmentation rates, like those for α-decarboxylation, also vary in a patterned way with changes in arene ring, nitrogen, and α- and *β*-carbon substituents. An investigation of the dynamics of methanol-promoted reactions of α-(trimethylsilyl)methyl-substituted anilinium radicals, has demonstrated that a change in the nitrogen substituent from alkyl to acyl causes an ca. 10-fold increase in the desilylation rate. Parallel photochemical studies have been conducted to gain chemical evidence to support assignment of the anilinium radical decay pathways in the LFP experiments and to demonstrate the preparative consequences of the kinetic results. First, clean formation of products derived by coupling of the (*N*-methylanilino)methyl radical in photochemical reactions of 1,4-dicyanobenzene with either tetra-*n*-butylammonium *N*-methyl-*N*-phenylglycinate or *β*-(*N*-methyl-*N*-phenyl)aminoethanol shows that the respective decarboxylation and retro-aldol cleavage processes occur with exceptionally high efficiencies. Second, in accord with the high rates observed for aminium radical decarboxylation and base-induced retro-aldol fragmentation, tethered cyclohexenone−α-aminocarboxylates and −*β*-aminoethanols undergo high-yielding SET-promoted photocyclization reactions under both direct and SET-sensitized conditions. Last, results which depict how the rates of aminium radical α-fragmentation correlate with quantum efficiencies of SET-promoted reactions of tertiary amines and amides have come from a study of photocyclization reactions of *N*-(aminoethyl)- and (amidoethyl)phthalimides. The quantum yields for these SET-promoted processes are observed to vary with the electrofugal group and nitrogen substituent in the manner predicted on the basis of the LFP-determined fragmentation rates.

Introduction

Ion radicals serve as key intermediates in a large number of ground-state and excited-state redox reactions. As a result, knowledge about the chemical properties of these short-lived species leads to a greater understanding of the detailed mechanisms of those redox reactions which are initiated by single electron transfer (SET).[2] Also, information about the properties associated with the charge and odd electron characters of ion radical intermediates can foster the rational design of new and, in some cases, synthetically important redox processes.[3] Although the current level of knowledge about the chemistry of anion and cation radicals is high,[4] much less is known about the dynamics of even the most common reactions of these intermediates despite the fact that these data are of central importance to predicting and controlling the efficiencies of SET-promoted reactions. The relevance of ion radical reaction dynamics to this issue is readily demonstrated by use of the hypothetical photoinduced SET process given in Scheme 1. It can be seen that the rates of the two cation radical reactions (k_1

[†] University of New Mexico.
[‡] University of Maryland.
[§] Pusan National University.

(1) A major portion of the studies reported in this paper was conducted as part of the doctoral work of Z.S. at the University of Maryland, and a preliminary communication reporting some of the results of the laser flash photolysis study has appeared (Su, Z.; Falvey, D. E.; Yoon, U. C.; Mariano, P. S. *J. Am Chem. Soc.* **1997**, *119*, 5261).

(2) (a) Mann, C. K.; Barnes, K. K. *Electrochemical Reactions in Non-Aqueous Systems*; Marcel-Dekker: New York, 1970. (b) Fox, M. A., Chanon, M., Eds. *Photoinduced Electron Transfer*; Elsevier: New York, 1988.

(3) Mariano, P. S. *Tetrahedron* **1983**, *39*, 3845. Mariano, P. S. *Synthetic Organic Photochemistry*; Horspool, W. M., Ed.; Plenum Press: London, 1984.

(4) (a) Chanon, M.; Rajzmann, M.; Chanon, F. *Tetrahedron* **1990**, *46*, 6193. (b) Schmittel, M.; Burghart, A. *Angew Chem., Int. Ed. Engl.* **1997**, *36*, 2550.

10.1021/ja981541f CCC: $15.00
Published on Web 10/01/1998

Scheme 1

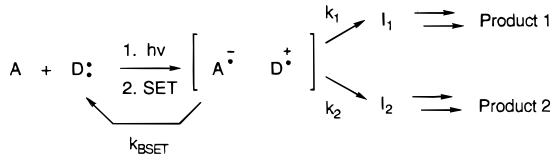

and k_2) govern both the relative yields of product 1 and product 2 ($1/2 \propto k_1/k_2$) as well as the quantum efficiency (ϕ) for product formation ($\phi \propto [k_1 + k_2]/[k_1 + k_2 + k_{BSET}]$).

Amine cation radicals (aminium radicals) are among the most interesting members of the charged radical family owing to the role they play as intermediates in oxidation reactions of amines. The chemical reactivity of these transients governs the nature and efficiencies of a variety of processes initiated by SET photochemical,[5] metal cation,[6] electrochemical,[7] and enzymatic[8] oxidation.

The most common reaction pathway followed by aminium radicals involves base-promoted deprotonation at either nitrogen (for primary (1°) and secondary (2°) aminium radicals) or the α-carbon (for tertiary (3°) aminium radicals).[5] The kinetics of these acid−base reactions were investigated originally by using product distribution techniques.[5,9] More recently, reliable data on the rates of α-CH deprotonation reactions of 3° aminium radicals (eq 1) have come from direct measurements by use of

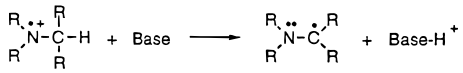

(1)

pulse radiolysis,[10] stopped-flow,[11] electrochemical,[12] and laser flash photolysis (LFP) techniques.[13] In addition, these studies have yielded information about how the rates of α-CH deprotonation are affected by base strength, α-isotopic substitution, and substituents at the nitrogen and α-carbon centers.

From a synthetic perspective, SET-oxidations of 3° amines can be used as a method to generate both α-amino radicals and iminium cations (Scheme 2). These intermediates, having opposite charge affinity profiles, participate in interesting C−C bond-forming reactions with respective electron-poor and electron-rich alkenes.[14] The yields of these processes when conducted on complex molecular systems can be severely compromised by (1) the lack of regioselectivity associated with an unselective aminium radical deprotonation step and (2) the comparable rates of oxidation of the reactant and product amines. Fortunately, there exist other types of α-fragmentation reactions of 3° aminium radicals which can serve as potentially more selective surrogates for the α-deprotonation process.[9,14,15]

Scheme 2

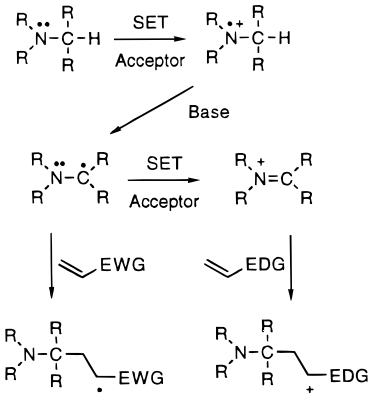

Included in this general family are the α-decarboxylation,[16] α-desilylation,[15] and α-retro-aldol[17] cleavage reactions shown in eqs 2−4. However, little[18] is known about the dynamics of these reactions and, equally significant, how the rates of these fragmentations are governed by factors (e.g., solvents, additives, N-blocking groups) which can be experimentally manipulated.

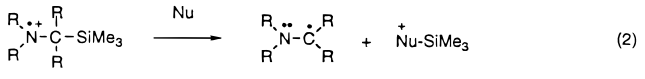

(2)

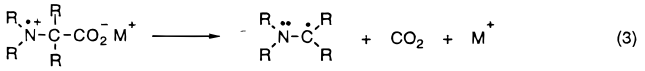

(3)

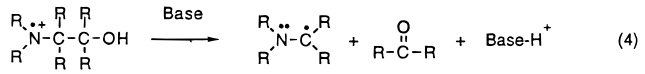

(4)

The aim of the investigation described below was to determine the rates of the common aminium radical fragmentation reactions, to delineate how the rates vary with solvents, additives, and substituents, and to assess the significance of the rate data in terms of the design of selective and efficient photoinduced SET oxidation reactions of amines.[1]

Results

Laser Flash Photolysis Studies. Earlier,[13] we showed that laser flash excitation of tertiary anilines in the presence of the electron acceptor 1,4-dicyanobenzene (DCB) leads to production of spectroscopically detectable anilinium radicals whose decay kinetics could be quantitatively analyzed. This SET sensitization technique is employed in the current study to generate tertiary anilinium radicals from designed series of α-anilinocarboxylates **1**−**7**, β-anilinoethanols **8**−**15**, and α-anilinotrimethylsilanes **16**−**18**. The decay kinetics of anilinium radicals derived from each of these substances has been measured and analyzed in terms of respective decarboxylation, retro-aldol cleavage, and α-desilylation reactions which result in formation of corresponding

(5) Lewis, F. D. *Acc. Chem. Res.* **1986**, *19*, 401. See also: Pienta, N. J. *Photoinduced Electron Transfer*; Fox, M. A., Chanon, M., Eds.; Elsevier: New York, 1988; Part C.

(6) Zhang, X. M.; Mariano, P. S.; Fox, M. A.; Martin, P. S.; Merkert, J. *Tetrahedron Lett.* **1993**, *34*, 5239. Castro, P.; Overman, L. E.; Zhang, X. M.; Mariano, P. S. *Tetrahedron Lett.* **1993**, *34*, 5243.

(7) Yoshida, K. *Electrooxidations in Organic Chemistry*; Wiley: New York, 1984.

(8) Van Houten, K. A.; Kim, J. M.; Bogdan, M.; Ferri, D. C.; Mariano, P. S. *J. Am. Chem. Soc.* **1998**, *120*, 5864.

(9) Xu, W.; Mariano, P. S. *J. Am. Chem. Soc.* **1991**, *113*, 1431. Xu, W.; Zhang, X. M.; Mariano, P. S. *J. Am. Chem. Soc.* **1991**, *113*, 8863.

(10) Das, S.; von Sonntag, C. Z. *Naturforsch.* **1986**, *416*, 505.

(11) Dinnocenzo, J. P.; Banach, T. E. *J. Am. Chem. Soc.* **1989**, *111*, 8646.

(12) Parker, V. D.; Tilset, M. *J. Am. Chem. Soc.* **1991**, *113*, 8778.

(13) Zhang, X.; Yeh, S. R.; Hong, S.; Freccero, M.; Albini, A.; Falvey, D. E.; Mariano, P. S. *J. Am. Chem. Soc.* **1994**, *116*, 4211.

(14) Jeon, Y. T.; Lee, C. P.; Mariano, P. S. *J. Am. Chem. Soc.* **1991**, *113*, 8863.

(15) Yoon, U. C.; Mariano, P. S. *Acc. Chem. Res.* **1992**, *25*, 233.

(16) Davidson, R. S.; Steiner, P. R. *J. Chem. Soc. (C)* **1971**, 1682. Davidons, R. S.; Harrison, K.; Steiner, P. R. *J. Chem. Soc. (C)* **1971**, 3480. Davidson, R. S.; Orton, S. P. *J. Chem. Soc. Chem. Communm.* **1974**, 209. See also: Battacharyya, S. M.; Das, P. K. *J. Chem. Soc., Faraday Trans.* **1984**, *80*, 1107.

(17) Gaillard, E. R.; Whitten, D. G. *Acc. Chem. Res.* **1996**, *29*, 292.

(18) (a) This is not true for the retro-aldol cleavage process which has been subjected to thorough kinetic studies by Schanze and co-workers (ref 18b) and to a lesser extent the desilylation process which has been the subject of preparative photochemical studies (refs 9, 14, and 15). (b) Burton, R. D.; Bartberger, M. D.; Zhang, Y.; Eyler, J. R.; Schanze, K. S. *J. Am. Chem. Soc.* **1996**, *118*, 5655. Lucia, L. A.; Burton, R. D.; Schanze, K. S. *J. Phys. Chem.* **1993**, *97*, 9078.

Table 1. Second-Order Rate Constants (k_{BSET}) for Decay of the Respective Cation and Anion Radicals Derived from the Anilines **22**−**24** and DCB at 25 °C

		$k_{BSET} \times 10^{-10}$ (M^{-1} s^{-1})[a]					
solvent	viscosity (η)	**22**	DCB	**23**	DCB	**24**	DCB
EtOH	108	3.5 ± 0.2	4.3 ± 0.1	1.1 ± 0.1	1.0 ± 0.1	5.6 ± 0.2	5.4 ± 0.2
MeOH	55	4.7 ± 0.1	4.8 ± 0.3	1.2 ± 0.1	1.1 ± 0.1	6.1 ± 0.1	6.2 ± 0.1
MeCN	35	6.0 ± 0.1	6.5 ± 0.4	1.5 ± 0.1	1.6 ± 0.1	6.5 ± 0.1	7.3 ± 0.4
mixture[b]		5.6 ± 0.1	6.2 ± 0.2	1.3 ± 0.1	1.5 ± 0.1	6.2 ± 0.2	6.9 ± 0.3

[a] Error limits were obtained by use of three to five independent experiments each. [b] MeCN−MeOH, 60:40 v/v.

α-anilino radicals (eq 5). The aniline derivatives used in this study were prepared by the straightforward procedures described in Supporting Information.

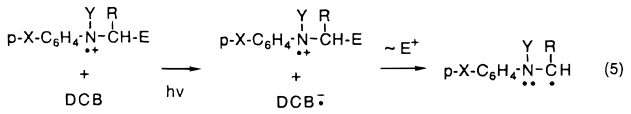

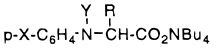

	X	Y	R
1	H	Me	H
2	OMe	Me	H
3	CF_3	Me	H
4	H	CO_2Et	H
5	H	COMe	H
6	H	Me	Me
7	H	Me	Ph

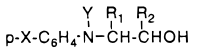

	X	Y	R_1	R_2
8	H	Me	H	H
9	OMe	Me	H	H
10	CF_3	Me	H	H
11	H	CD_3	H	H
12	H	Me	H	Ph
13	OMe	Me	H	Ph
14	H	Me	Me	H
15	H	Me	Ph	H

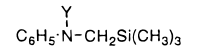

	Y
16	Me
17	CO_2Et
18	COMe

Calibration of the LFP Systems. Initial studies were conducted with the aniline derivatives **19**−**24** to allow comparison of the results of this effort with those obtained from our earlier work.[13] Laser excitation (308 nm, 6 ns, 50−60 mJ) of deoxygenated solutions of each of these aniline derivatives in polar solvents including MeOH, EtOH, and MeCN containing DCB (50 mM) leads to generation of two transients characterized as the corresponding anilinium radical (430−480 nm)[19] and DCB anion radical[20] (330 nm). Analysis of the decay profiles by use of a second-order treatment (see eq 6 in the Experimental Section) and known extinction coefficients[19,20] gives the rate constants for bimolecular decay of these transients (representative data in Table 1).

Scheme 3

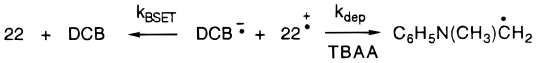

Table 2. Second-Order Rate Constants (k_{dep}) for TBAA-Induced α-CH Deprotonation of the Cation Radicals Derived from Anilines **19**−**24** in MeCN at 25 °C

aniline	k_{dep} (M^{-1} s^{-1})	aniline	k_{dep} (M^{-1} s^{-1})
19	2.0×10^5	**22**	$(1.3 \pm 0.2) \times 10^5$
20	8.0×10^4	**23**	2.2×10^4
21	8.9×10^5	**24**	2.7×10^5

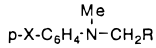

	X	R
19	H	H
20	MeO	H
21	CF_3	H
22	H	CO_2Et
23	MeO	CO_2Et
24	CF_3	CO_2Et

In each case, decay rates for the anilinium radicals and DCB anion radical partners are nearly equivalent and dependent on solvent viscosity. These observations are consistent with the assignment of diffusion governed back electron transfer as the major pathway for decay of the transients in the absence of added base. In addition, para substituents appear to influence the back-SET rates in the order OMe < H < CF_3.

An alternate mode of anilinium radical decay, involving α-CH deprotonation, is introduced when the base, (^{n}Bu)$_4$NOAc (TBAA), is present in the solution subjected to LFP. The dependence of the 460-nm transient decay rate on TBAA concentration is used to determine the anilinium radical second-order deprotonation rate constants. Accordingly, flash irradiation of solutions containing each of the anilines **19**−**24**, DCB, and TBAA along with (^{n}Bu)$_4$NClO$_4$ (TBAP) to maintain a constant ionic strength of 0.5 M gives rise to transient anilinium radicals whose decays are kinetically analyzed by using the mixed second-order (BSET)−pseudo-first-order (acetate-promoted deprotonation) mechanistic sequence shown in Scheme 3 (see eq 7 in the Experimental Section). This treatment gives pseudo-first-order rate constants (k_{obs}) for TBAA-induced decay. Plots of k_{obs} vs TBAA concentration yields slopes from which the second-order rate constants (k_{dep}) for TBAA-induced α-deprotonation of the anilinium radicals are calculated (Table 2).

The α-CH deprotonation rate constants for the anilinium radicals derived from **19**−**21** are close to those previously determined,[13] thus establishing the integrity of the current

(19) Arimitsu, A.; Masuhara, N.; Mataga N. *J. Phys. Chem.* **1975**, *79*, 1255.

(20) Robinson, E. A.; Schulte-Frohlinde, D. *J. Chem. Soc., Faraday Trans.* **1973**, *69*, 707.

Table 3. Second-Order Rate Constants (k_{BSET}) for Decay of the Ion Radicals from LFP of the β-Anilinoethanols **8**−**10** and DCB at 25 °C

	$k_{BSET} \times 10^{-10}$ (M^{-1} s^{-1})[a]					
solvent	**8**	DCB	**9**	DCB	**10**	DCB
EtOH	1.2	1.2	0.9	1.1	1.2	1.3
MeOH	1.6	1.3	1.2	1.2	1.7	1.8
MeCN	2.3	2.3	2.0	1.8	2.1	2.8
mixture[b]	2.2	2.1	1.4	1.4	1.8	2.6

[a] Maximum error limits of $\pm 0.1 \times 10^{10}$ were determined by use of three to five independent experiments. [b] MeCN−MeOH, 60:40 v/v.

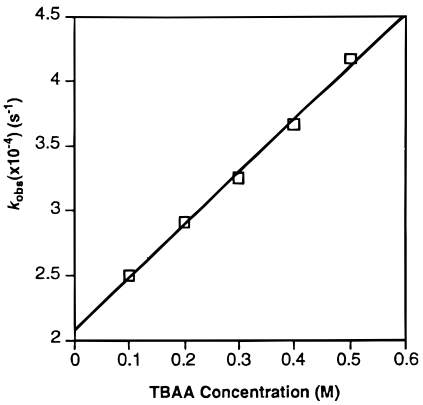

Figure 1. Plot of the observed rate constant for decay of the β-anilinoethanol **8** cation radiacal vs TBAA concentration in 60:40 MeOH−MeCN at 25 °C.

experimental system. The small differences (e.g., for $\mathbf{1}^{\bullet+}$ 2.0 $\times$ 10^5 M^{-1} s^{-1} (current) vs 3.1 $\times$ 10^5 M^{-1} s^{-1} (previous)) between the current and previous data are a result of the use of a mathematical model comprised of a mixed second-order−pseudo-first-order decay treatment (Scheme 3) in this work as compared to an inferior one which was used earlier.[13]

Anilinium Radical Retro-Aldol Cleavage Kinetics. The LFP methodology discussed above is employed to determine the decay kinetics of cation radicals derived by SET-sensitized photolysis of the β-anilinoethanol derivatives **8**−**15**. In each case, decay of the anilinium radical intermediates in the absence of base occurs by back electron transfer with bimolecular rate constants which again depend on the solvent viscosity and para substituents (Table 3).

The rates of decay of the cation radicals derived by one-electron oxidation of the β-anilinoethanols depend in a linear fashion on the concentration of the base, TBAA. The observed pseudo first-order rate constants for acetate-promoted decay of these transients at various TBAA concentrations and constant ionic strength of 0.5 M (maintained with TBAP) are determined by use of the competitive second-order (BSET)−pseudo-first-order (acetate-promoted deprotonation) decay sequence like that shown in Scheme 3 (see eq 7 in the Experimental Section). Plots of k_{obs} vs TBAA concentration (e.g., Figure 1) yield the second-order rate constants (k_{ra}) listed in Table 4 for TBAA-promoted decay of the β-anilinoethanol cation radicals.

The new pathway for TBBA-promoted decay of the anilinoethanol cation radicals is attributed to retro-aldol cleavage. This conclusion is based on the results of deuterium isotope labeling and preparative photochemical studies. The rate constant for bimolecular decay of the OD isotopomer of $\mathbf{8}^{\bullet+}$ (measured in 60:40 MeOD−MeCN) is 9.0 $\times$ 10^3 M^{-1} s^{-1}, which corresponds to an OD isotope effect of 2.2. In addition, the CD_3 derivative **11** was prepared and subjected to LFP study. Analysis of the dependence of k_{obs} for decay of $\mathbf{11}^{\bullet+}$ as a function of TBAA concentration gives the small CD_3 isotope effect of 1.3. Both observations are inconsistent with a mechanism involving α-CH deprotonation of the anilinoethanol cation radicals since a near-zero OD isotope effect and large α-CD_3 isotope effect[13] would have been expected (see below).

Table 4. Second-Order Rate Constants (k_{ra}) for TBAA-Promoted Retro-Aldol Cleavage of the Cation Radicals Derived from **8**−**15** in MeCN at 25 °C

anilinoethanol	k_{ra} (M^{-1} s^{-1})[a]	anilinoethanol	k_{ra} (M^{-1} s^{-1})[a]
8	$(4.1 \pm 0.6) \times 10^4$	**12**	3.1×10^5
9	$(2.8 \pm 0.3) \times 10^4$	**13**	2.0×10^5
10	3.1×10^5	**14**	3.3×10^4
11	3.2×10^4	**15**	$(3.8 \pm 0.7) \times 10^5$

[a] Error limits were obtained by use of three to five independent experiments.

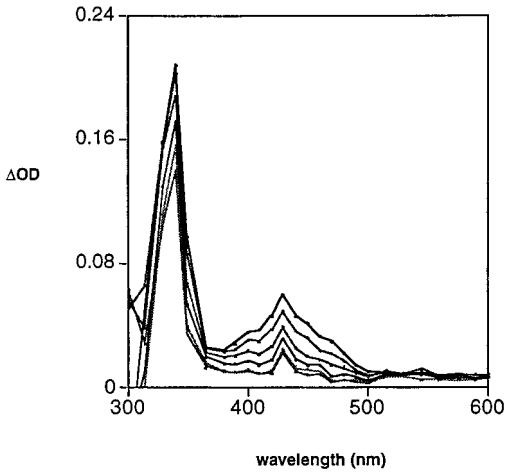

Figure 2. Transient absorption spectra following (1, 2, 5, 10, and 40 μs) 308-nm excitation of and MeCN (25 °C) solution of **1** (0.5 mM) and DCB (50 mM).

Anilinium Radical α-Decarboxylation Kinetics. An initial concern in our studies with α-anilinocarboxylates **1**−**7** is the question of whether SET-photosensitized oxidation of these substrates occurs at the tertiary amine center rather than at the carboxylate moiety. Two factors suggested that anilinium rather than carboxy radical formation would be favored in these systems. In the LFP experiment with excitation at 308 nm, the primary light absorbing species is the anilinocarboxylate and not the electron acceptor, DCB. Thus, the pathway for ion radical production involves SET from the excited aniline chromophore to the ground state of DCB. In addition, the oxidation potentials of carboxylates are generally in the range 1.2−1.5 V,[21] while those of tertiary anilines are ca. 0.3−0.8 V.[22] Thus, even if equilibration of the anilinium and carboxy radicals occurs following the initial SET event, the former species would be thermodynamically favored.

As expected, LFP excitation (308 nm) of an MeCN (25 °C) solution of anilinocarboxylate **1** (0.5 mM) containing 50 mM DCB leads to generation of transients absorbing at 340 and 450−480 nm, characteristic of the respective ion radicals of $DCB^{\bullet-}$ and $\mathbf{1}^{\bullet+}$ (e.g., Figure 2). The decay profiles of the intermediates (e.g., Figure 3) show that the anilinium radicals disappear at much greater rates than that of $DCB^{\bullet-}$. Thus, in

(21) Eberson, L. *Chemistry of the Carboxyl Group*; Patai, S., Ed.; Wiley: London, 1969; Chapter 2. Torii, S.; Tanaka, H. *Organic electrochemistry*; Lund, H., Baiter, M. M., Eds.; Marcel Dekker: New York, 1991; Chapter 14.

(22) Cf. Miller, L. L.; Nordblum, G. D.; Mayeda, E. A. *J. Org. Chem.* **1972**, *37*, 916. Yoshida, J.; Isoe, S. *Tetrahedron Lett.* **1987**, *28*, 6621. Cooper, B. E.; Owen, W. *J. Organomet. Chem.* **1971**, *29*, 33.

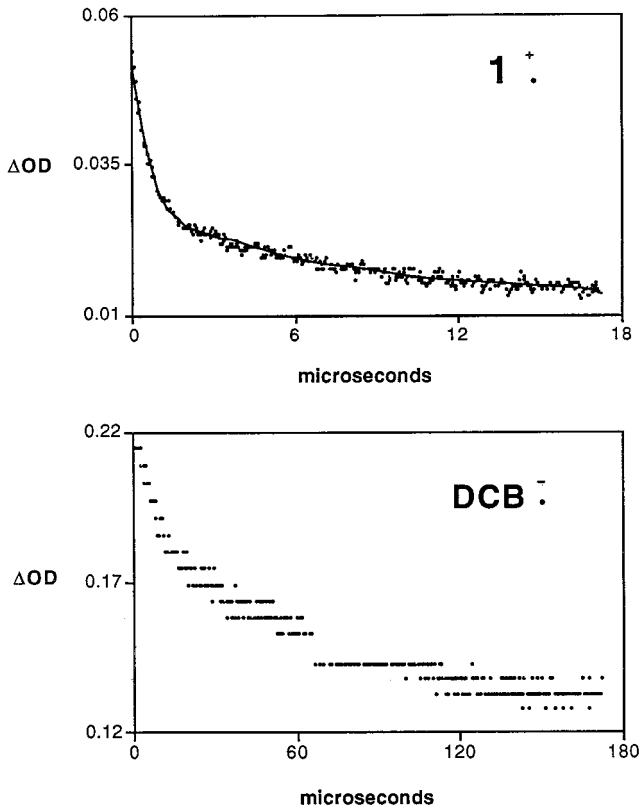

Figure 3. Decay profiles for the ion radicals of **1** and DCB obtained from the LFP experiment described in Figure 2.

Scheme 4

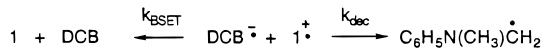

Table 5. First-Order Rate Constants (k_{dec}) for Decarboxylation of the Cation Radicals Derived from the α-Anilinocarboxylates **1**−**7** in MeCN at 25 °C

α-anilino-carboxylate	k_{dec} (s^{-1})[a]	α-anilino-carboxylate	k_{dec} (s^{-1})[a]
1	$(1.7 \pm 0.2) \times 10^6$	**5**	3.6×10^7
2	$(8.2 \pm 0.3) \times 10^5$	**6**	1.3×10^6
3	1.3×10^7	**7**	2.6×10^6
4	2.8×10^7		

[a] Error limits were determined by use of three to five independent experiments.

this system, back electron transfer is not a major reaction pathway involved in the decay of the anilinium radicals. Thus, kinetic treatments of the decay of the anilinium radicals by use of either the competitive first-order ($-CO_2$)−second-order (BET) sequence shown in Scheme 4 (see eq 7 in the Experimental Section) or a first-order process (correcting for comparably slow BET, see eq 8 in the Experimental Section) both give excellent fits of the data and equivalent (within experimental error) first-order decay rate constants (k_{dec}) attributed to unimolecular α-decarboxylation (see below). This experimental method and the ensuing kinetic treatments when applied to a series of para-, nitrogen-, and α-carbon-substituted α-anilinocarboxylates give the decarboxylation rate data included in Table 5.

Additional information about the anilinium radical decarboxylation process is gained from studies probing the effects of solvent and added salts. As seen by inspecting the data given in Table 6, solvent polarity has a small but patterned effect on the rate of the decarboxylation reaction of the anilinium radical,

Table 6. Solvent Polarity Effects on the Decarboxylation Rates of the Anilinium Radical of **1**

solvent	$E_T(30)$[a]	k_{dec} (s^{-1}) (25 °C)[b]
MeOH	55.5	2.8×10^6
EtOH	51.9	2.5×10^6
MeCN	46.7	$(1.7 \pm 0.2) \times 10^6$
60:40 MeOH−MeCN		1.9×10^6

[a] Dimroth, K.; Reichardt, C.; Siepmann, T.; Bohlmann, F. *Ann. Chem.* **1963**, *661*, 1. [b] Error limits were determined by use of three independent experiments.

Table 7. Metal Cation Effects on the Decarboxylation Rates of the Anilinium Radical of **1**

salt	concn (mM)	$k_{dec} \times 10^{-6}$ (s^{-1}) (25 °C, MeCN)	salt	concn (mM)	$k_{dec} \times 10^{-6}$ (s^{-1}) (25 °C, MeCN)
$^nBu_4NClO_4$	1	2.4	$CsClO_4$	1	4.1
$^nBu_4NClO_4$	10	1.2	$CsClO_4$	10	2.9
$^nBu_4NClO_4$	100	0.5	$CsClO_4$	100	0.3
$LiClO_4$	10	1.1	$Mg(ClO_4)_2$	1	0.15
$NaClO_4$	10	1.9	$Mg(ClO_4)_2$	10	0.12
$KClO_4$	10	2.5	$Ca(ClO_4)_2$	1	0.15
$RbClO_4$	10	2.8	$Ca(ClO_4)_2$	10	0.08

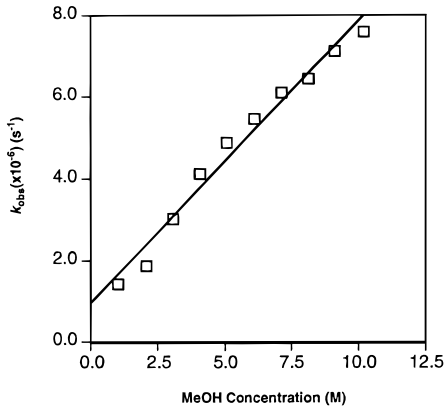

Figure 4. Plot of the observed rate constant for decay of the cation radical of anilinosilane **16** vs MeOH concentration in MeCN at 25 °C.

1$^{\bullet+}$. In addition, metal perchlorate salts also influence the kinetics of this process. LFP experiments were conducted with MeCN (25 °C) solutions of **1** (0.5 mM) and DCB (50 mM) containing varying concentrations of the salts listed in Table 7. Two trends appear to be associated with the data. First, k_{dec} decreases as the concentration of the added salt increases and the magnitude of the effect increase in proceeding from salts with small, monovalent metal cations to those with large, divalent metal cations.

Anilinium Radical α-Desilylation Kinetics. In an earlier effort,[13] we determined the second-order rate constants for MeOH-, H_2O-, and $^nBu_4NF$-promoted α-desilylation of the anilinium radical arising by SET-sensitized laser excitation of the α-anilinosilane **16**. As a consequence of the effects of the N-substituent on the rates of anilinium radical retro-aldol cleavage and decarboxylation seen in this study (see Tables 4 and 5), the desilylation process was reinvestigated. Irradiation (308 nm) of MeCN (25 °C) solutions of **16**−**18** (0.5 mM) and DCB (50 mM) containing varying concentrations of MeOH followed by employment of a competitive second-order (BSET)−pseudo-first-order (MeOH promoted desilylation) kinetic treatment (see eq 7 in the Experimental Section) leads to the observed desilylation rate constants. A plot of k_{obs} vs MeOH concentration (e.g., Figure 4) yields the second-order rate

Table 8. Second-Order Rate Constants (k_{Des}) for MeOH-Assisted Desilylation of α-Anilinosilane **16**−**18** Derived Cation Radicals in MeCN at 25 °C

α-anilinosilane	k_{des} (M^{-1} s^{-1})[a]	α-anilinosilane	k_{des} (M^{-1} s^{-1})[a]
16	7.0×10^5	**18**	$6.0 \pm 1.0 \times 10^7$
17	1.8×10^7		

[a] The error limit was determined by use of three independent experiments.

Scheme 5

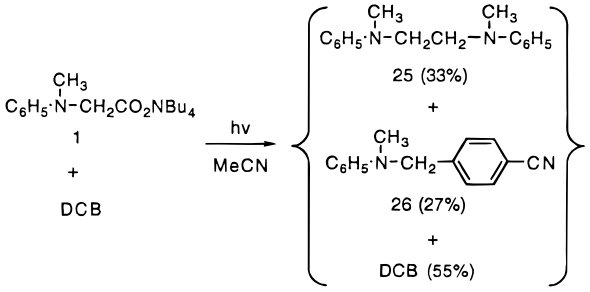

Scheme 6

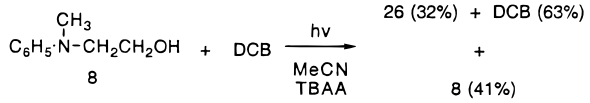

constants for MeOH-promoted desilylation (k_{des}) of the α-silylanilinium radicals (Table 8).

Preparative Photochemical Studies. Photoreactions of α-Anilinocarboxylate 1 and *β*-Anilinoethanol 8 with DCB. To connect the observations made in the LFP effort to real intermediates and decay pathways, preparative photochemical reactions of the α-anilinocarboxylate **1** and *β*-anilinoethanol **8** with DCB were conducted under conditions which mimic, as best as possible, those existing in the laser excitation experiments. Accordingly, an MeCN solution of **1** (2.5 mM) and DCB (2.5 mM) is irradiated with Pyrex filtered light ($\lambda > 290$ mm). An exceptionally clean reaction ensues when the reactant conversion is ca. 50%. Chromatographic separation affords the diamine **25** (30%) and cyanobenzylaniline **26** (27%) along with recovered DCB (55%) (Scheme 5).

In a similar fashion, low-conversion irradiation of **8** (2.4 mM) in an MeCN solution containing both DCB (2.4 mM) and TBAA (0.3 M) followed by chromatographic separation gives the cyanobenzylaniline **26** (32%) along with recovered DCB (63%) and **8** (41%) (Scheme 6).[23]

The outcomes of these preparative photochemical processes are in full accord with the conclusion that the major if not exclusive mechanistic pathways followed in the SET photoreactions of the α-anilinocarboxylates and *β*-anilinoalcohols involve respective decarboxylation and retro-aldol cleavage of intermediate cation radicals. Both α-fragmentation reactions lead to production of α-anilinomethyl radicals which undergo either self-coupling to form diamine **25** or addition to the DCB anion radical to provide the cyanobenzylaniline **26**. The differences between the **25** and **26** product ratios in these photoprocesses is interesting and is discussed below.

Photocyclization Reactions of Aminocarboxylate- and Aminoethanol-Substituted Cyclohexenones. Earlier,[8,9,14] we demonstrated the synthetic potential of SET-promoted photocyclization reactions of aminoalkyl-substituted, conjugated ketones and esters which follow either direct (diradical coupling) or SET-sensitized (radical addition) pathways. The results highlighted the importance of aminium radical α-heterolytic fragmentation in governing both the efficiencies and regioselectivities of the cyclization processes. For example, photoreactions of α-silylaminoenones **28** (Scheme 7) lead to selective and high-yielding formation of non-silicon-containing products **27** owing to the larger rates of MeOH-induced desilylation vs intramolecular deprotonation of intermediate aminium radicals. In contrast, irradiation of these same substrates in MeCN yields silicon-containing products **29** which arise by α-deprotonation of the nitrogen-centered cation radical intermediates.

Scheme 7

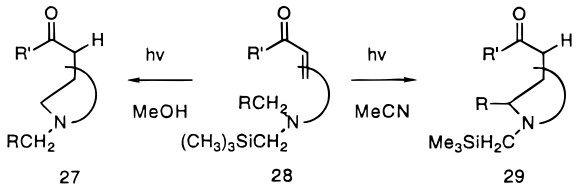

Scheme 8

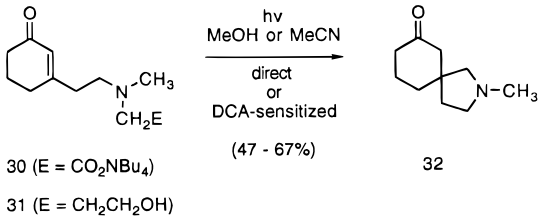

The results of the LFP studies described above suggest that SET-promoted photocyclization reactions of α-aminocarboxylate tethered conjugated ketones in MeCN should favor pathways in which decarboxylation rather than deprotonation of intermediate aminium radicals occurs. Likewise, conjugated ketones containing aminoethanol substitution should also undergo photocyclization reactions in the presence of the base, TBAA, which are characterized by selective retro-aldol fragmentation of amine cation radical intermediates. These predictions are fully supported by observations made in studies of the preparative photochemistry of cyclohexenones **30** and **31** (Scheme 8). For example, irradiation of the aminocarboxylate **30** in MeCN or MeOH under either direct or 9,10-dicyanoanthracene (DCA) sensitized conditions leads to efficient formation of the spriocyclic ketone **32**. In a similar manner, **32** is formed in the direct and SET-sensitized photoreactions of aminoethanol **31**. Finally, DCA-sensitized irradiation of the analogous carbamidocarboxylates **33** and **35** promotes efficient formation of the respective bicyclic ketones **34** and **36** via pathways involving formation and decarboxylation of intermediate carbamate cation radicals (Scheme 9).

Quantum Efficiencies of *N*-(Aminoethyl)phthalimide Photocyclization Reactions. The rates of aminium radical α-heterolytic fragmentation also can govern the quantum efficiencies of SET-promoted photoreactions of amine substrates. In these processes, fragmentation in the direction of product formation competes with energy-wasting back electron transfer to regenerate the ground-state starting substrate. Thus, aminium radical fragmentation rates should correlate with the quantum yields of SET photoreactions conducted under identical conditions within a regular series of amine substrates. Results which demonstrates this relationship and show how electrofugal group and N-substituent selection can be used to optimize quantum

(23) (a) Schuster, I. I. *J. Org. Chem.* **1985**, *50*, 1656. (b) Robinson, E. A.; Schulte-Frohlinde, D. *J. Chem. Soc., Faraday Trans. 1* **1973**, 707. (c) Albini, A.; Fasani, E.; Oberti *Tetrahedron* **1982**, *38*, 1034. Lewis, F. D.; Petisce, J. R. *Tetrahedron* **1986**, *42*, 6207.

Scheme 9

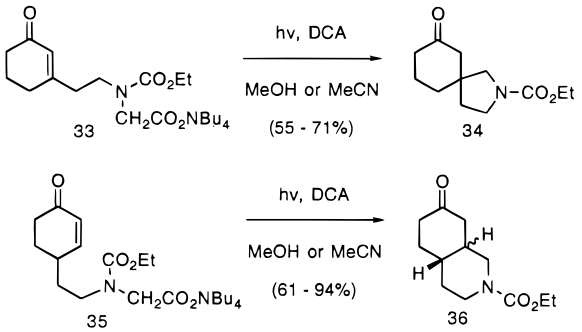

Scheme 10

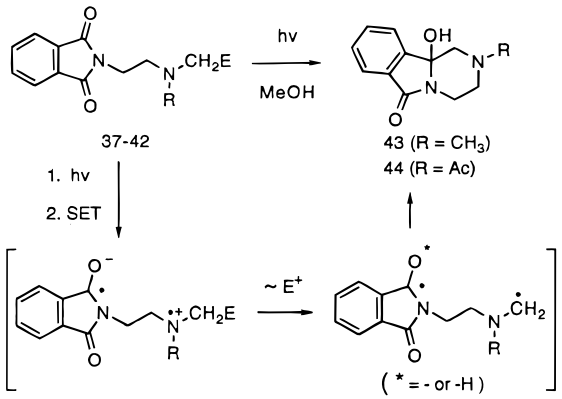

efficiencies have come from quantitative studies with the *N*-(aminoethyl)phthalimides **37**−**42**.

Photoreactions of phthalimides **37**−**42** occur by pathways involving initial SET from the amine-nitrogen center to the excited phthalimide followed by aminium radical fragmentation to generate the diradical precursor of the cyclic products (Scheme 10). As can be seen by viewing the data given in Table 9, quantum yields for photocyclization product formation vary in a regular manner with the LFP measured rates of *N*-alkyl- and *N*-acylaminium radical decay by desilylation, decarboxylation, and deprotonation.

Discussion

Anilinium Radical Decay Pathways. A general problem associated with the interpretation of LFP experiments that rely on observations of transient decay rates is the unambiguous assignments of chemical pathways to the decay processes. In the current effort, we have attempted to accumulate supporting evidence to enable firm assignments of α-decarboxylation and retro-aldol cleavage as the major, if not exclusive, mechanisms responsible for decay of anilinium radicals derived from the respective α-anilinocarboxylates and *β*-hydroxyanilines.

Preparative photochemistry often serves as a useful method to correlate transient decay routes with chemical mechanisms. An example is found in our earlier studies with α-silylamines. The fact that desilylation is the major pathway for LFP-detected α-silylanilinium radical decay is suggested by the observations that the decay rates show first-order dependences on the concentration of nucleophiles (e.g., ROH and F^-) and a direct dependence on the silophilicity of the nucleophiles (e.g., F^- > H_2O > MeOH > MeCN). This conclusion is strongly supported by results emanating from preparative photochemical studies[14,15] which demonstrate that the major products of α-silylamine SET photoreactions occurring in silophilic solvents arise by desilylation-promoted generation and secondary reaction of α-amino radical intermediates (see Scheme 7).

Table 9. Quantum Efficiencies for SET-Promoted Photocyclizations of the (Aminoethyl)- and (Amidoethyl)phthalimides **37**−**42**

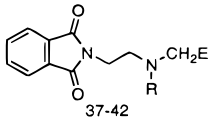

phthalimide	R	E	additive	ϕ^a
37	Me	H	TBAA	0.003
38	Ac	H	TBAA	0.025
39	Me	TMS	TBAP	0.038
40	Ac	TMS	TBAP	0.12
41	Me	CO_2NBu_4	TBAP	0.32
42	Ac	CO_2NBu_4	TBAP	0.40

[a] All photoreactions were conducted on MeOH solutions containing added TBAA (0.3 M) or TBAP (0.3 M) at 25 °C. Conversions are between 5 and 20%. Quantum efficiencies are reported as averages of three independent measurements and errors range from ±0.0001 to ±0.007.

Scheme 11

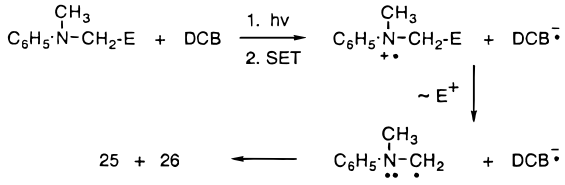

Earlier observations made by Davidson[16] indicate that aminium radicals produced by SET oxidation of α-aminocarboxylates and *β*-aminoalcohols decay by decarboxylation and retro-aldol fragmentation routes. Later studies of the *β*-aminoalcohol cation radical fragmentation process have been conducted by Whitten and co-workers.[17] The results of our current work provide further support for these proposals in the context of the specific systems probed in the LFP effort. Accordingly, SET-promoted preparative photoreactions of the anilinocarboxylate **1** and anilinoethanol **8** with DCB both occur in near quantitative yield to generate products of direct (**25**) and cross (**26**) coupling of the α-anilinomethyl radical intermediate. Therefore, α-decarboxylation and retro-aldol cleavage must be the exclusive processes responsible for anilinium radical decay in the mechanistic sequences for production of **25** and **26**, from **1** and **8** (Scheme 11).

A number of factors could be responsible for the different **25**:**26** product ratios observed in these reactions. For example, TBAA-promoted retro-aldol fragmentation of $\mathbf{8}^{\bullet+}$ produces acetic acid as a consequence of hydroxyl proton transfer to acetate. Consequently, protonation or hydrogen bonding[23a] of HOAc to the base $DCB^{\bullet-}$ [23b] is likely in this case. In this case, the **25**:**26** product ratio is then governed by the relative rates of α-anilino radical coupling with itself vs the dicyanohydrophenyl radical DCB−H$^\bullet$ or H-bonded $DCB^{\bullet-}$. In contrast, decarboxylation of $\mathbf{1}^{\bullet+}$ does not produce an acid, and as a result, the **25**:**26** distribution is controlled by the rates of α-anilino radical self-coupling vs its addition to $DCB^{\bullet-}$. It should be mentioned in this regard that Albini and Lewis[23c] have independently observed effects of added trifluoroacetic acid and trifluoroethanol on the ratios of products formed in SET-promoted photoreactions of toluene derivatives with polycyanoarenes and have rationalized these results in terms of hydrogen bonding to or protonation of the intermediate cyanoarene anion radicals.[23]

Equally relevant to this issue are the photocyclization reactions of tethered aminoenone systems (Schemes 8 and 9) which are driven by the same aminium radical fragmentation processes. For example, the DCA-photosensitized transformations of aminocarboxylate **30** and aminoalcohol **31** to spirocyclic amino ketone **32** occur by routes in which selective decarboxylation and retro-aldol cleavage of the aminium radical intermediates sets the stage for the key α-amino radical cyclization steps.

Relative Rates of Retro-Aldol vs α-Deprotonation. Inspection of the rate data included in Tables 2 and 4 reveals a curious, yet understandable, feature of the kinetics of TBAA-promoted α-CH deprotonation and retro-aldol cleavage processes. Accordingly, bimolecular α-CH deprotonation rates for the *N*,*N*-dialkylanilium radicals derived from **19**−**24** are larger than those for bimolecular retro-aldol cleavage of comparably substituted *β*-hydroxyanilinium radicals [**8**−**15**$^{\bullet+}$]. This comparison leads one to question (1) if retro-aldol cleavage is really the process involved in the LFP-determined transient decay processes of [**8**−**15**$^{\bullet+}$], and (2) if so, why retro-aldol fragmentation is faster than α-CH deprotonation in the anilinium radicals which bear a *β*-hydroxyl group.

Additional information was accumulated to substantiate the operation of TBAA-induced retro-aldol fragmentation rather than α-CH deprotonation pathways for decay of the transients arising by SET-photosensitized irradiation of the *β*-hydroxyanilines **8**−**15**. If retro-aldol cleavage is the major or exclusive pathway for anilinium radical decay in these systems, a large primary OD isotope effect (ca. **2**)[24] would be expected. Also, since anilinium radical α-CH deprotonation is kinetically preferred at α-CH_3 vs α-CH_2−R centers,[13,25] a large primary α-CD_3 isotope effect (ca. **3**)[13] would be anticipated if this mechanism is responsible for transient decay. The data recorded for the OD analogue of **8**$^{\bullet+}$ and CD_3 analogue **11**$^{\bullet+}$ demonstrate that TBAA-induced decay of the *β*-hydroxyanilinium radicals is associated with large (2.2) OD and small (1.3) α-CD_3 isotope effect. Thus, the preparative photochemical and kinetic isotope effect results leave little doubt that retro-aldol cleavage is faster than α-CH deprotonation in *β*-hydroxyanilinium radicals.

On the basis of these results, it is reasonable to conclude that *β*-hydroxyanilinium radicals are intrinsically less reactive than their non-hydroxyl-bearing analogues. Relevant to this issue are observations which show that cation radicals derived from properly structured tertiary diamines exist as through-space, three-electron N−N-bonded structures[26a] and that "tied-back" tertiary aminium radicals form three-electron-bonded dimers with neutral tertiary amines.[26b] Thus, it may be generally true that tertiary aminium radicals can be stabilized by weak, through-space, three-electron-bond interactions with neighboring groups which bear nonbonded electrons. Interactions of this type between the aminium radical and *β*-hydroxyl centers (e.g., **45**) would lead to stabilization of *β*-hydroxyanilinium radicals

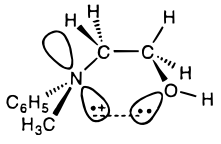

45

and, consequently (see below), to reduced rates of their TBAA-promoted α-CH deprotonation and retro-aldol cleavage reactions. It should be noted that an explanation of this type is in full accord with the suggestion made by Schanze[18b] that *β*-hydroxyl stabilization is responsible for the smaller rate of pyridine induced retro-aldol fragmentation of threo vs erthryo *β*-hydroxy-α,*β*-diphenylethylanilinium radicals.

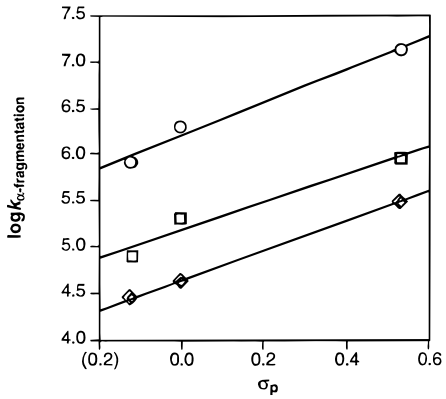

Figure 5. Linear-free energy plot of the log of the rate constants for decarboxylation (circles), deprotonation (squares), and retro-aldol cleavage (diamonds) reactions of anilinium radicals vs σ_p values of the *p*-phenyl substituents, MeO, H, and CF_3.

Electrofugal Group and Substituent Effects on Aminium Radical Fragmentation Rates. In our earlier efforts,[13] we showed that *p*-phenyl substituents play a significant role in determining the rates of TBAA-induced anilinium radical α-CH deprotonation. The current data indicates that parallel substituent effects exist for both the decarboxylation and retro-aldol cleavage reactions of anilinium radicals. A simple linear free energy treatment of the data (Figure 5) yields *ρ* values for deprotonation, decarboxylation, and retro-aldol cleavage of 1.5, 1.8, and 1.6, respectively. The near equality of these values demonstrates that the transition states of all three fragmentation processes have similar charge and odd-electron distributions.

As we[13] and others[27] have discussed, rates of the anilinium and related cation radical α-CH deprotonation reactions parallel thermodynamic acidities. Thus, the rates are directly proportional to the oxidation potentials[28] of the amine precursors or, said in another way, inversely related to the thermodynamic stabilities of the aminium radicals. Since *N*-acyl substituents have a large effect on the oxidation potentials of amines, one would predict that the rates of α-heterolytic fragmentation of amide-derived cation radicals would be greater than those of their amine analogues. Indeed, the large increases in the rates of anilinium radical decay caused by changes from *N*-alkyl to *N*-acyl substituents are observed for all of the fragmentation processes investigated.

The results of this study also provide some information about the effects of α-C substituents on the rates of the α-heterolytic fragmentation reactions. In anilinium radical α-CH deprotonation,[13] retro-aldol cleavage, and decarboxylation reactions,

(24) Schanze and co-workers have reported an OD isotope effect of 2.0 for pyridine-promoted retro-aldol fragmentation of the anilinium radical derived from the 2-(*N*-phenylamino)-1,2-diphenylethanols (ref 18b).

(25) Lewis, F. D.; Ho, T. I.; Simpson, J. T. *J. Am. Chem. Soc.* **1986**, *104*, 1924. Lewis, F. D.; Ho, T. I.; Simpson, J. T. *J. Org. Chem.* **1981**, *46*, 1077.

(26) (a) Kirste, B.; Alder, R. W.; Sessions, R. B.; Bock, M.; Kurreck, H.; Nelsen, S. F. *J. Am. Chem. Soc.* **1985**, *107*, 2635. (b) Dinnocenzo, J. P.; Banach, T. E. *J. Am. Chem. Soc.* **1988**, *110*, 971.

(27) (a) Anne, A.; Fraoua, S.; Grass, V.; Moiroux, J.; Saveant, J.-M. *J. Am. Chem. Soc.* **1998**, *120*, 2951 and references therein. (b) Schlesener, C. J.; Amatore, C.; Kochi, J. K. *J. Am. Chem. Soc.* **1984**, *106*, 3567, 7472. Masanovi, J. M.; Sankaraman, S.; Kochi, J. K. *J. Am. Chem. Soc.* **1989**, *111*, 2263.

(28) Nicholas, A. P. M.; Arnold, D. R. *Can. J. Chem.* **1982**, *60*, 2166. Nicholas, A. P. M.; Boyd, R. J.; Arnold, D. R. *Can. J. Chem.* **1982**, *60*, 3011.

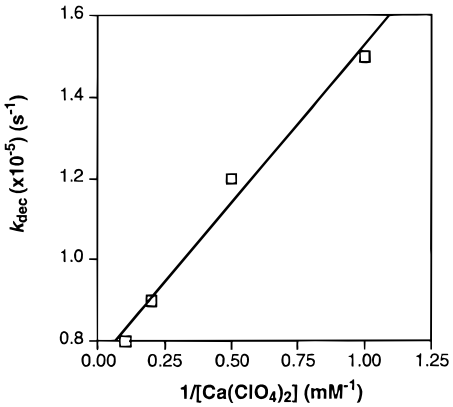

Figure 6. Plot of the rate of unimolecular decarboylation of $\mathbf{1}^{\bullet+}$ in MeCN at 25 °C vs the reciprocal of $Ca(ClO_4)_2$ concentration.

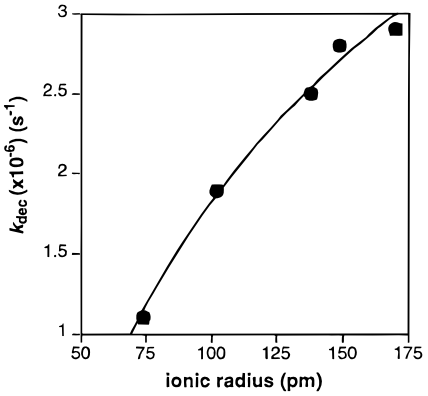

Figure 7. Plot of the rate constant for decarboxylation of $\mathbf{1}^{\bullet+}$ in MeCN at 25 °C containing 10 mM $MClO_4$ (M = Li, Na, K, Cs, and Rb) vs the ionic radius of M^+ (Keer, J. A. *Chem. Rev.* **1966**, *66*, 465. Janz, G. J. *Thermodynamic Properties of Organic Compounds*; Academic Press: New York, 1993).

α-methyl substitution leads to decreased fragmentation rates whereas α-phenyl substitution leads to increased rates. It appears that the rationale put forth by Lewis[25] for α-substituent effects on the rates of aminium radical α-CH deprotonations (i.e., that they are governed by a combination of steric/steroelectronic (σ_{C-E}⁻p_{N}•⁺ overlap) and electronic (α-amino radical stabilization) holds for all related processes in which an electrofugal group is lost or transferred from an α-position.

From the perspective of preparative photochemistry, the substituent effects on the rates of aminium radical fragmentations can be used advantageously in the design of more highly quantum efficient processes operating via SET pathways. Observations made in studies of the (aminoethyl)phthalimide photocyclization reactions exemplify this feature. Specifically, the results demonstrate that the quantum yields are qualitatively related to the LFP measured rates of aminium radical fragmentation. The preparative utility of the LFP rate data is further exemplified by the observation that the inefficient photocyclization of phthalimide **37** can be transformed into exceptionally efficient photoreaction by simply changing the electrofugal group from H to CO_2NBu_4 and the N-substituent from methyl to acetyl.

Medium and Metal Cation Effects on the Rates of α-Decarboxylation of Anilinium Carboxylates. Owing to the potential relevance of the anilinium radical decarboxylation process to the design of fast unimolecular processes for α-amino radical initiated polymerizations, we probed this reaction in greater detail. The results provide useful information about how medium and countercation influence the rates of these processes. As seen by viewing the data in Table 6, the rates of decarboxylation of the ammonium carboxylate $\mathbf{1}^{\bullet+}$ vary slightly, yet in a patterned way (log $k_{dec} \propto E_T$) with changes in the polarity of the solvent. Also, the presence of metal perchlorate salts results in a reduction of the $\mathbf{1}^{\bullet+}$ decarboxylation rates and this effect displays well-behaved metal cation concentration (Figure 6), ionic radius (Figure 7), and charge/radius dependencies.

These observations can be explained by use of the simple mechanistic model shown in Scheme 12. The anilinium carboxylate in solution can exist as two limiting structures, represented by the free zwitterion **46** and ion paired form **47**. Which of these structural extremes best represents the major anilinium carboxylate produced in the SET step should be governed by solvent polarity and oxophilicity of the metal cation (e.g., **46** should dominate in more highly polar solvents and when M^+ is a large monovalent cation). In addition, decarboxylation of the free zwitterion **46** should occur at a faster rate than that of the ion-paired intermediate **47**. Contributing to this is the fact that loss of CO_2 in **47** requires rupture of the metal−oxygen bond and a larger reorganization of the ion pairing and solvation interactions.

Scheme 12

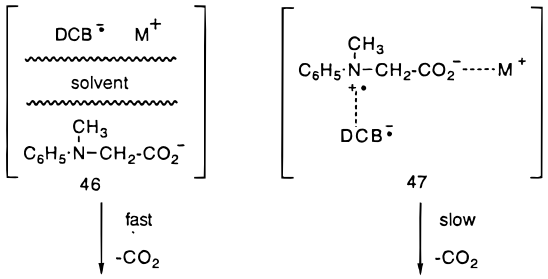

Conclusions

The issues associated with aminium radical α-heterolytic fragmentation processes discussed above have been addressed in this study by using a combination of photophysical and photochemical methods. An SET photosensitization technique in conjunction with time-resolved laser spectroscopy has been employed to generate and kinetically analyze the decay processes of anilinium radicals derived by one-electron oxidation of α-anilinocarboxylates, *β*-anilinoalcohols, and α-anilinosilanes. In this manner, we determined that the rates of unimolecular decarboxylation of anilinium carboxylate radicals are in the range 10^6-10^7 s^{-1} and are dependent upon solvent polarity, the metal cation, and substituents on the aniline ring, nitrogen, and α-carbon. In addition, kinetic analysis of base-induced retro-aldol fragmentations of cation radicals arising by SET oxidation of *β*-anilinoalcohols has shown that bimolecular rate constants vary from 10^4 to 10^5 M^{-1} s^1 and are close to those for α-deprotonation reactions of related *N*,*N*-dialkylanilinium radicals. The retro-aldol fragmentation rates such as those for α-decarboxylation reactions also vary in a patterned way with changes in arene ring, nitrogen, and α- and *β*-carbon substituents. In an extension of an earlier investigation of the dynamics of methanol-promoted reactions of α-(trimethylsilyl)methyl anilinium radicals, we have found that changes in the nitrogen substituent have a profound effect on α-desilylation rates.

Parallel photochemical studies have been conducted both to gain chemical evidence to support assignment of the anilinium radical decay pathways and to demonstrate the preparative consequences of the kinetic results. First, clean formation of products derived by coupling of the (*N*-methylanilino)methyl

radical in photochemical reactions of 1,4-dicyanobenzene with either tetra-*n*-butylammonium *N*-methyl-*N*-phenylglycinate or *β*-*N*-methyl-*N*-phenylaminoethanol shows that the respective decarboxylation and retro-aldol cleavage processes occur with exceptionally high efficiencies. Second, in accord with the high rates observed for aminium radical decarboxylation, tethered cyclohexenone−α-aminocarboxylates undergo high-yielding SET-promoted photocyclization reactions under both direct and SET-sensitized conditions. Last, we have demonstrated how the rates of aminium radical α-fragmentation correlate with quantum efficiencies of SET-promoted reactions of tertiary amines and amides. A study of photocyclization reactions of *N*-(aminoethyl)- and (amidoethyl)phthalimides show that the quantum yields for these SET-promoted processes vary with the electrofugal group and nitrogen substituent in the manner predicted on the basis of the LFP-determined α-fragmentation rates.

Experimental Section

General Procedure. All reported reactions were run under a dried nitrogen atmosphere. Unless otherwise noted, all reagents were obtained from commercial sources and used without further purification. Dimethyl sulfoxide and triethylamine were distilled from calcium hydride. Anhydrous solvents were obtained by distillation from the indicated reagents: ether (Na, benzophenone ketyl), tetrahydrofuran (Na, benzophenone ketyl), methylene chloride (P_2O_5). Column chromatography was performed with silica gel (230−400 mesh), Florisil (100−200 mesh) adsorbents, or alumina (neutral, 80−120 mesh). Preparative TLC was performed on 20 × 20 cm plates coated with silical gel. All compounds were isolated as oils and shown to be >90% pure by ^{1}H and/or ^{13}C NMR unless otherwise noted.

^{1}H NMR and ^{13}C NMR spectra were recorded by using $CDCl_3$ solutions unless otherwise specified, and chemical shifts are reported in parts per million relative to residual $CHCl_3$ at 7.24 ppm (for ^{1}H NMR) and 77.0 ppm (for ^{13}C NMR). ^{13}C NMR resonance assignments were aided by the use of the DEPT technique to determine numbers of attached hydrogens, and ^{1}H NMR coupling constants (*J* values) are reported in hertz. Infrared spectra were obtained neat liquids unless otherwise specified, and data are reported in units of cm^{-1}. Low (MS) and high (HRMS) mass spectra, reported as *m*/*z* (relative intensity), were recorded by using electron impact ionization (EI) unless otherwise specified as chemical ionization (CI) or fast atom bombardment ionization (FAB).

Photochemical reactions were conducted by using an apparatus consisting of a 450-W medium-pressure mercury lamp surrounded by a Pyrex or uranium glass filter and within a quartz, water-cooled well that was purged with O_2-free N_2 both before and during irradiation. Photochemical reaction progress was monitored by gas chromatography, TLC, or ^{1}H NMR. The solvents used in the photoreactions were spectrograde: MeCN (Baker) or MeOH (Baker). 1,4-Dicyanobenzene (DCB) was purchased from Aldrich and recrystallized ($CHCl_3$) prior to use. 9,10-Dicyanoanthracene (DCA) was purchased from Eastman Kodak and recrystallized from benzene.

Photoaddition of DCB to the Anilinocarboxylate 1. A deoxygenated MeCN solution (20 mL) containing **1** (20 mg, 0.049 mmol) and DCB (6 mg, 0.049 mmol) was irradiated with Pyrex glass filtered light for 20 min. The photolyzate was diluted with water and extracted with ether. The ethereal extracts were dried and concentrated in vacuo, and the residue was subjected to column chromatography (silica gel, 20% ether/hexanes) to yield 2 mg (30%) of *N*,*N*′-dimethyl-*N*,*N*′-diphenylethylene-1,2-diamine (**25**) and 3 mg (27%) of *N*-(4-cyanobenzyl)-*N*-methylaniline (**26**) with 4 mg (55%) of recovered DCB.

25: ^{1}H NMR (CD_3CN) 2.89 (s, 6H, $2NCH_3$), 3.51 (s, 4H, $2NCH_2$), 6.60−6.71 (m, 6H, aromatic), 7.12−7.21 (m, 4H, aromatic); ^{13}C NMR (CD_3CN) 38.8 (NCH_3), 50.1 (NCH_2), 112.8, 116.8, 118.9 and 130.1 (aromatic); IR 2957, 2925, 2863, 1733, 1599, 1506, 1374, 747, 692; MS 241 (3), 240 (15), 149 (22), 120 (100), 105 (12), 91 (5), 77 (10); HRMS calcd for $C_{16}H_{20}N_2$ 240.1626, found 240.1626.

26: ^{1}H NMR (CD_3CN) 3.04 (s, 3H, NCH_3), 4.60 (s, 2H, NCH_2), 6.60−6.71 (m, 3H, aromatic), 7.11−7.20 (m, 2H, aromatic), 7.36 and 7.65 (ABq, J = 8.3, 4H, aromatic); ^{13}C NMR (CD_3CN) 39.4 (NCH_3), 56.7 (NCH_2), 113.2, 117.5, 119.7, 128.5, 130.1, 133.3, 146.6 and 150.2 (aromatic), 180.1 (CN); IR 2919, 2360, 1599, 1506, 1347, 1251, 934, 749, 691; MS 223 (15), 222 (86), 221 (24), 120 (100), 116 (23), 106 (24), 105 (12), 91 (14), 77(35); HRMS calcd for $C_{15}H_{14}N_2$ 222.1157, found 222.1159.

Photoaddition of DCB to the Aminoalcohol 8. A deoxygenated MeCN solution (100 mL) containing **8** (36 mg, 0.24 mmol), DCB (31 mg, 0.24 mmol), and tetrabutylammonium acetate (TBAA) (9.04 g, 30.0 mmol) was irradiated with Pyrex glass filtered light for 2 h. The photolyzate was concentrated under reduced pressure to ca. 20 mL. The mixture was diluted with water and extracted with ether. The ethereal extracts were dried and concentrated in vacuo, and the residue was subjected to column chromatography (silica gel, 20% ether/hexanes) to yield 17 mg (32%) of **26** and 3 mg of an unknown with 15 mg (41%) of **8** and 19 mg (63%) of recovered DCB.

Photochemistry of Aminoenone 30. A deoxygenated MeCN solution (100 mL) containing **30** (150 mg, 0.33 mmol) was irradiated with uranium glass filtered light for 4 h. The photolyzate was concentrated to ca. 5 mL, diluted with water, and extracted with ether. The ethereal extracts were dried and concentrated in vacuo. The residue was subjected to preparative TLC separation (silica gel, 66% ether/hexanes) to yield 34 mg (61%) of the spirocyclic amino ketone **32:** ^{1}H NMR 1.55−1.64 (m, 2H), 1.69−1.75 (m, 2H), 1.74−1.85 (m, 2H), 2.18−2.31 (m, 5H), 2.25 (s, 3H, NCH_3), 2.34 (d, J = 9.3, 1H), 2.46−2.54 (m, 2H); ^{13}C NMR 23.3 (C_7), 36.9 (C_4 or C_6), 37.6 (C_6 or C_4), 41.0 (C_8), 42.1 (NCH_3), 46.9 (C_5), 54.5 (C_{10}), 55.7 (C_3), 68.0 (C_1), 210.6 (C═O); MS 167 (13), 130 (35), 109 (10), 96 (20), 70 (15), 58 (46), 57 (100); HRMS calcd for $C_{10}H_{17}NO$ 167.1310, found 167.1311.

A MeOH solution (100 mL) containing **30** (150 mg, 0.33 mmol) was irradiated with uranium glass filtered light for 5 h. Workup and preparative TLC separation (silica gel, 66% ether/hexanes) furnished 32 mg (58%) of **32**.

An MeCN solution (100 mL) containing **30** (150 mg, 0.33 mmol) and DCA (8 mg, 0.033 mmol) was irradiated with uranium glass filtered light for 4 h. Workup followed by preparative TLC separation (silica gel, 66% ether/hexanes) provided 33 mg (59%) of **32**.

A MeOH solution (20 mL) containing **30** (25 mg, 0.055 mmol) and DCA (3 mg, 0.011 mmol) was irradiated with uranium glass filtered light for 5 h. Workup followed by preparative TLC separation (silica gel, 66% ether/hexanes) gave 6 mg (63%) of **32**.

Photochemistry of Aminoenone 31. An MeCN solution (100 mL) containing **31** (100 mg, 0.51 mmol) and TBAA (3.0 g, 10 mmol) was irradiated with uranium glass filtered light for 7 h. The photolyzate was concentrated under reduced pressure to give a residue which was subjected to column chromatography (silica, ether). The ethereal eluent was concentrated under reduced pressure to give a residue which was subjected to preparative TLC separation (silica gel, 75% ethyl acetate/hexanes) to yield 40 mg (47%) of **32**.

A MeOH solution (20 mL) containing **31** (20 mg, 0.10 mmol) and TBAA (1.5 g, 5 mmol) was irradiated with uranium glass filtered light for 10 h. Workup and preparative TLC separation (silica gel, 66% ether/hexanes) furnished 10 mg (62%) of **32**.

An MeCN solution (100 mL) containing **31** (100 mg, 0.51 mmol), TBAA (3.0 g, 10 mmol), and DCA (12 mg, 0.052 mmol) was irradiated with uranium glass filtered light for 8 h. Workup followed by preparative TLC separation (silica gel, 66% ether/hexanes) provided 54 mg (64%) of **32**.

A MeOH solution (20 mL) containing **31** (20 mg, 0.10 mmol), TBAA (1.5 g, 5 mmol), and DCA (2.5 mg, 0.011 mmol) was irradiated with uranium glass filtered light for 9 h. Workup followed by preparative TLC separation (silica gel, 66% ether/hexanes) gave 10 mg (58%) of **32**.

DCA-Sensitized Irradiation of 33. An MeCN solution (100 mL) containing **33** (190 mg, 0.37 mmol) and DCA (21 mg, 0.09 mmol) was irradiated with uranium glass filtered light for 10 h. The photolyzate was concentrated under reduced pressure to give a residue. This residue was dissolved in 10 mL of methanol and filtered. The filtrate was diluted with water and extracted with ether. The ethereal

extracts were dried and concentrated in vacuo. The residue was subjected to preparative TLC separation (silica gel, 50% hexanes/acetone) to yield 59 mg (71%) of **34**. ^{1}H NMR 1.23 (t, J = 7.0, 3H, OCH_2CH_3), 1.70−1.80 (m, 4H), 1.84−1.89 (m, 2H), 2.30−2.35 (m, 4H), 3.15, 3.22 (s, 2H, H_1), 3.39−3.44 (m, 2H), 4.09 (q, J = 7.0, 2H, OCH_2CH_3); ^{13}C NMR 14.8 (OCH_2CH_3); 23.1, 23.2 (C_7), 33.9 (C_6 or C_4), 35.8, 35.9 (C_4 or C_6), 40.1 (C_8), 44.1, 44.4 (C_{10}), 45.5, 46.5 (C_5), 50.3, 50.4 (C_3), 55.8, 56.6 (C_1), 61.1 (OCH_2CH_3), 155.1 (NCO_2Et), 209.9 ($O{=}C_9$); IR 2940, 2872, 1700, 1424, 1381, 1347, 1227, 1115, 770; MS 226 (6), 225 (31), 180 (13), 168 (14), 167 (100), 152 (14), 116 (27), 115 (39), 93 (25), 82 (21), 67 (29); HRMS calcd for $C_{12}H_{19}NO_3$ 225.1365, found 225.1368.

A MeOH solution (100 mL) containing **33** (190 mg, 0.37 mmol) and DCA (21 mg, 0.09 mmol) was irradiated with uranium glass filtered light for 5 h. Workup and preparative TLC separation (silica gel, 50% hexanes/acetone) gave 46 mg (55%) of **34**.

DCA-Sensitized Irradiation of 35. An MeCN solution (100 mL) containing **35** (150 mg, 0.29 mmol) and DCA (17 mg, 0.074 mmol) was irradiated with uranium glass filtered light for 7 h. The photolyzate was concentrated under reduced pressure to give a residue. This residue was dissolved in 5 mL of methanol and filtered. The filtrate was diluted with water and extracted with ether. The ethereal extracts were dried and concentrated in vacuo. The residue was subjected to preparative TLC separation (silica gel, 30% hexanes/ether) to yield 19 mg (41% based on the conversion) of *cis*-**36** and 24 mg (53% base on the conversion) of *trans*-**36** with 47 mg (31%) of recovered **35**.

***cis*-36:** ^{1}H NMR 1.18 (t, J = 7.0, 3H, OCH_2CH_3), 1.45−2.40 (m, 11H), 3.00−3.20 (m, 2H), 3.54−3.70 (m, 1H), 4.09 (q, J = 7.0, 2H, OCH_2CH_3); ^{13}C NMR 14.7 (OCH_2CH_3); 25.6, 29.4 (C_4, C_5), 33.0 (C_{4a}, C_{8a}), 37.4 (C_6), 41.7 (C_8), 42.2 (C_3), 47.4 (C_1), 61.4 (OCH_2CH_3), 155.9 (NCO_2Et), 211.2 ($O{=}C_7$); IR 2980, 2934, 2865, 1697, 1435, 1239, 1122, 769; MS 225 (7), 196 (5), 180 (5), 168 (13), 167 (100), 154 (16), 152 (14), 116 (14); HRMS calcd for $C_{12}H_{19}NO_3$ 225.1365, found 225.1361.

***trans*-36:** ^{1}H NMR 1.18 (t, J = 7.1, 3H, OCH_2CH_3), 1.45−2.50 (m, 11H), 3.00−3.20 (m, 2H), 3.58−3.60 (m, 1H), 4.11 (q, J = 7.1, 2H, OCH_2CH_3); ^{13}C NMR 14.6 (OCH_2CH_3); 25.4, 29.7 (C_4, C_5), 33.0 (C_{4a}, C_{8a}), 37.4 (C_6), 41.6 (C_8), 42.8 (C_3), 47.4 (C_1), 61.4 (OCH_2CH_3), 155.9 (NCO_2Et), 211.2 ($O{=}C_7$); IR 2939, 2855, 1697, 1436, 1239, 1123, 769; MS 226 (6), 225 (12), 168 (14), 167 (100), 154 (18), 152 (14), 122 (10), 116 (44), 95 (12); HRMS calcd for $C_{12}H_{19}NO_3$ 225.1365, found 225.1356.

A MeOH solution (100 mL) containing **35** (150 mg, 0.29 mmol) and DCA (17 mg, 0.074 mmol) was irradiated with uranium glass filtered light for 6 h. Workup and preparative TLC separation (silica gel, 30% hexanes/ether) gave 14 mg (26% based on the conversion) of *cis*-**36**, 19 mg (35% base on the conversion) of *trans*-**36** with 27 mg (18%) of recovered **35**.

Quantum Yields for Photoreactions of Phthalimides 37−42. Quantum yields were measured by using 300-nm light and a 0.10 M benzophenone−benzhydrol actinomer. Individual methanol solutions (10 mL) containing phthalimides **37** (31 mg, 14.0 mM) and **38** (17 mg, 6.99 mM), **39** (98 mg, 33 mM) and **40** (107 mg, 34 mM), and **41** (92 mg, 35 mM) and **42** (200 mg, 69 mM) all in sealed tubes were simultaneously irradiated with 300-nm light to affect ca. 5−20% conversions. The crude photolyzates were analyzed by UV spectroscopy at 300 nm to determine phthalimide conversions. Quantum yields listed in Table 9 are for photoproduct formation, calculated on the basis of starting phthalimide coversion and photocyclization product yield.

Laser Flash Spectroscopy Experiments. The laser kinetic experiments were performed by using a Questek 2120 excimer laser as the excitation source. All of the spectra and kinetic runs obtained were done using XeCl reagent gas which provides UV pulses at 308 nm with a duration of 6−10 ns and a pulse energy of 30−50 mJ. Transient UV/vis absorption signals were monitored using a CW 450-W Xe Arc Lamp beam which was passed through the sample perpendicular to the excitation beam. Single-wavelength transient wave forms were digitized using a LeCroy 9420 350-M digital oscilloscope and transferred to a Macintosh IIcx computer for storage and analysis.

Sample solutions were placed in 10 × 10 mm quartz cuvettes which were sealed with a rubber serum cap and purged with N_2 for 10−15 min prior to the experiment. Sample concentrations were adjusted such that their optical densities were 1.0−1.5 at the excitation wavelength (308 nm). The transient absorption spectra were detected in the 300−800-nm range.

Three mathematical expressions corresponding to the kinetic models for anilinium radical decay by BET to $BDB^{\bullet-}$ (eq 6), competitive second-order back BET−first- or pseudo-first-order decarboxylation, TBAA-induced deprotonation and TBAA-induced retro-aldol cleavage and MeOH-induced desilylation (eq 7), and corrected (for slow BET to DCB•-, eq 8) first-order decarboxylation were establishd in Mac II MATLAB 1.2c and MATLAB 4.2c.1 to analyze the decay processes:

$$[\overset{+\bullet}{S}] = \frac{1}{k_{2nd\text{-}order}\,xt + 1/C_1} + C_2 \qquad (6)$$

$$[\overset{+\bullet}{S}] = \frac{e^{-k_{first\ order\ or\ pseudo\text{-}1st\text{-}order}xt}}{k_{2nd\text{-}order}\,xt + 1/C_1} + C_2 \qquad (7)$$

$$[\overset{+\bullet}{S}] = C_1 x e^{-k_{1st\text{-}order}\,xt} + C_2 x e^{-k'_{correct}\,xt} + C_3 \qquad (8)$$

Equation 6 was employed to fit the profiles monitored at 340 nm and/or 460 nm for BET-promoted second-order decay of the ion radicals derived from aniline derivatives **8**−**10** and **19**−**24** and DCB in the absence of base. This provides the second-order rate constants for both DCB anion radical decay and anilinium radical decay by BET.

Equation 7 was employed to fit the profiles monitored at 460 nm for respective TBAA-induced retroaldol cleavage and deprotonation of the aminium radicals derived from **8**−**11** and **19**−**24**. The second-order rate constant $k_{2nd-order}$ corresponding to BET was set to be equal to that obtained for the decay process occurring in the absence of base by using eq 6. For the respective TBAA- and MeOH-promoted decay of the aminium radicals from **12**−**15** and **16**−**18**, $k_{2nd-order}$ corresponding to back electron transfer between the anilinium radicals and the anion radical of DCB was set to be equal to the rate constant for diffusion in MeCN. The pseudo-first-order rate constants, $k_{pseudo-first-order}$, corresponding to acetate-promoted deprotonation and retro-aldol cleavage, or MeOH-promoted desilylation were measured at different TBAA and MeOH concentrations and plots of $k_{pseudo-first-order}$ vs TBAA or MeOH concentrations gave the respective second-order rate constants for anilinium radical decay by deprotonation, retro-aldol cleavage, or desilylation.

Equation 7 was also utilized to fit the profiles for decay of the anilinocarboxylate-derived anilinium radicals **1**−**7** monitored at 460 nm. The second-order rate constant, $k_{2nd-order}$, for BET to the anion radical of DCB was set to be equal to the rate constant for diffusion in MeCN. The first-order rate constants corresponding to decarboxylation were then calculated. Equation 8 treats the data as a sum of a fast first-order decay by decarboxylation corrected for by a term related to a much slower BET process. Although less rigorously derived, eq 8 was also employed to analyze the decay profiles for the anilinium radicals. Two rate constants, $k_{1st-order}$ and $k'_{correct}$, were obtained by use of eq 8, and the one corresponding to the faster (by ca. 1 order of magnitude) decay process was ascribed to decarboxylation. The first-order rate constant for decarboxylation calculated by use of either eq 7 or eq 8, as expected, were equivalent within experimental error.

Acknowledgment. The authors appreciate the financial support generously provided by the NSF (P.S.M., CHE-9707401 and INT-9796064; D.E.F., CHE-9521601), KOSEF (U.C.Y., 965-0300-002-2), CBM Postech, and the Korea Ministry for Education (U.C.Y., BSRI-97-3408).

Supporting Information Available: Experimental descriptions of the synthetic routes used to prepare the substances used in this study are described (41 pages, print/PDF). See any current masthead page for ordering information and Web access instructions.

JA981541F